

Frustrated Ising model on the garnet lattice

Takuya Yoshioka, Akihisa Koga and Norio Kawakami

Department of Applied Physics, Osaka University, Suita, Osaka 565-0871

(Received July 31, 2021)

We investigate a frustrated Ising spin system on the garnet lattice composed of a specific network of corner-sharing triangles. By means of Monte Carlo simulations with the heat bath algorithm, we discuss the magnetic properties at finite temperatures. It is shown that the garnet spin system with the nearest-neighbor couplings does not exhibit any magnetic transitions, yielding the large residual entropy at zero temperature. We also investigate the effect of the long-range dipolar interaction systematically to determine the phase diagram of the Ising model on the garnet lattice. We find that there appear a variety of distinct phases depending on the cutoff length of the long-range interaction, in contrast to the pyrochlore spin-ice systems.

KEYWORDS: spin ice, frustration, garnet lattice, Ising model

1. Introduction

Recently, geometrically frustrated spin systems have attracted much interest. One of the most remarkable examples is the Ising-spin system on the geometrically frustrated pyrochlore lattice, such as $\text{Dy}_2\text{Ti}_2\text{O}_7$ ¹⁻⁶ and $\text{Ho}_2\text{Ti}_2\text{O}_7$.³⁻⁸ In these compounds, a magnetic moment located at each lattice point is quantized, due to strong easy-axis anisotropy, along the line joining the tetrahedra that compose the basic unit of the pyrochlore lattice. Strong geometrical frustration on this lattice yields remarkable properties quite analogous to the real ice, now called the *spin ice*:⁷ the system does not show any magnetic phase transitions, resulting in the finite residual entropy at zero temperature.^{1,5} It has been further confirmed that some portion of the residual entropy is released by an applied magnetic field, yielding another two-dimensional frustrated system on the Kagome lattice, which is now referred to as the *Kagome ice*.⁹⁻¹¹ More recently, it has been argued that the competition of the long-range dipolar interaction and the nearest neighbor superexchange interaction plays a crucial role to determine the magnetic properties in this class of frustrated Ising spin systems.^{6,8} These remarkable experimental observations of the spin-ice behavior have stimulated further intensive investigations in this field.

Motivated by these hot topics on spin-ice systems, we explore here another prototype of frustrated classical spin system, possessing the *garnet structure*, which is one of the most popular three-dimensional frustrated lattices. The garnet lattice is shown in Fig. 1 schematically, which is characterized by a specific network of corner-sharing triangles. In this sense, it should share some essential properties with the Kagome lattice formed by a two-dimensional network of corner-sharing triangles. Also, we expect that the system exhibits characteristic properties similar to the spin ice as observed in the pyrochlore compounds.¹⁻⁸

So far, classical Heisenberg models on the garnet lattice have been investigated, and the role of geometrical frustration has been discussed in connection with the compound $\text{Gd}_3\text{Ga}_5\text{O}_{12}$.¹²⁻¹⁴ In this paper, we focus on the Ising spin system, which should provide another in-

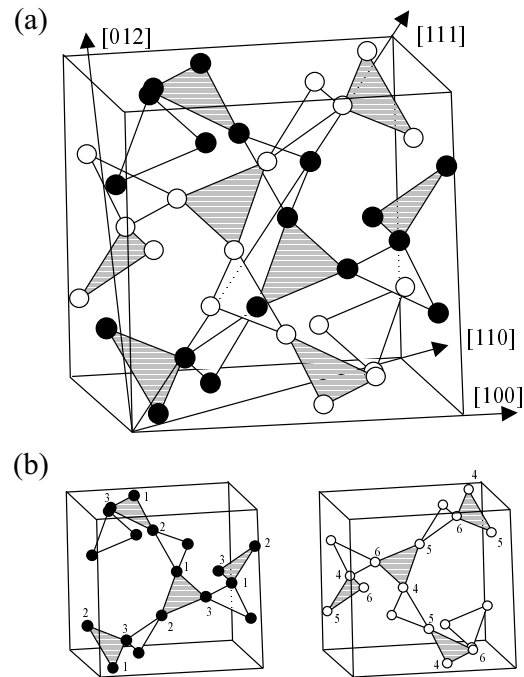


Fig. 1. (a) Garnet structure: there are twenty four sites in the unit cell. [100], [110], [111] and [012] represent the directions of the applied magnetic field (see text). (b) Two equivalent sublattices composing the garnet structure.

teresting aspect of frustration in the garnet lattice system. We shall indeed uncover that the garnet Ising system shows either spin-ice like behavior as the pyrochlore system, or magnetic phase transitions depending on the shape of the interactions. Although experimental study on the spin-ice behavior on the garnet lattice has not been reported so far, we expect that relevant compounds can be synthesized in the future, adding another interesting example to the class of spin-ice systems.

This paper is organized as follows. In §2, we introduce the Ising Hamiltonian on the garnet lattice, and briefly outline the numerical procedure. In §3, we first discuss the effects of frustration due to the nearest-neighbor exchange interaction to explore spin-ice like behavior, and

then investigate what kind of magnetic orders are stabilized by the long-range dipolar-type interaction. Brief summary is given in §4.

2. Model and Method

We investigate a frustrated Ising-spin model on the garnet lattice shown in Fig. 1. The garnet lattice composed of corner-sharing triangles possesses twenty-four spins in the unit cell. If one takes into account only the nearest neighbor interaction, the lattice is divided into two equivalent sublattices, as shown in Fig. 1 (b). In some kinds of frustrated spin systems, strong easy-axis anisotropy realizes the Ising spin system quantized in several distinct directions. In this paper, we assume strong easy-axis anisotropy along the line joining the triangular center, as realized in spin-ice pyrochlore systems.³ Define here the notation of scalar Ising spins: $\sigma_i = 1(-1)$ when a spin points outward (inward) of triangles drawn as the gray ones in Fig. 1 (a). The corresponding unit vector expressing the direction of the Ising spin is denoted as \mathbf{n}_i .

The Hamiltonian we consider here is

$$\mathcal{H} = \frac{1}{2} \sum_{i,j} [J_s \delta_{n.n.} + J_{ij}] \sigma_i \sigma_j - \sum_i \mu \sigma_i \mathbf{n}_i \cdot \mathbf{H},$$

$$J_{ij} = \frac{\mu_0 \mu^2}{4\pi} \left[\frac{\mathbf{n}_i \cdot \mathbf{n}_j}{r_{ij}^3} - 3 \frac{(\mathbf{n}_i \cdot \mathbf{r}_{ij})(\mathbf{n}_j \cdot \mathbf{r}_{ij})}{r_{ij}^5} \right], \quad (1)$$

where μ is the magnetic moment, J_s is the exchange interaction between nearest neighbor spins ($\delta_{n.n.}$ restricts the summation only for the nearest neighbors), J_{ij} is the dipolar interaction between two spins separated from each other by the distance r_{ij} , and \mathbf{H} is the magnetic field.

To investigate magnetic properties of the model, we make use of Monte Carlo simulations, where the heat bath method is used to realize the detailed balance. We perform the simulations for $L \times L \times L$ lattices ($24L^3$ lattice points) with $L = 5, 10, 15, 20$ by imposing periodic boundary conditions. To realize the equilibrium state, the simulation for the initial relaxation has been made with about 100,000 Monte Carlo steps per spin to obtain the expectation values for various static quantities such as the susceptibility, the specific heat and the entropy.

3. Results

We first discuss the effects of the nearest-neighbor exchange interaction J_s to observe how the spin-ice like properties show up in the Ising model on the garnet lattice. We then explore the competition between the nearest-neighbor interaction J_s and the long-range dipolar interaction J_{ij} , and determine the phase diagram of the model.

3.1 Garnet lattice with nearest neighbor interaction

We start with a garnet system with the nearest neighbor exchange interaction ($J_{ij} = 0$). Here, we assume the exchange coupling, $J_s > 0$, because the model with $J_s < 0$ without the dipolar interaction leads to a simple ordered phase. For later convenience, we introduce the effective coupling, $J_{n.n.} = J_s + J_{D1}$, where J_{D1} is

the dipolar interaction between nearest-neighbor spins. By performing Monte Carlo simulations for the system ($L = 10$), we estimate the temperature-dependent specific heat and entropy, as shown in Fig. 2. At high

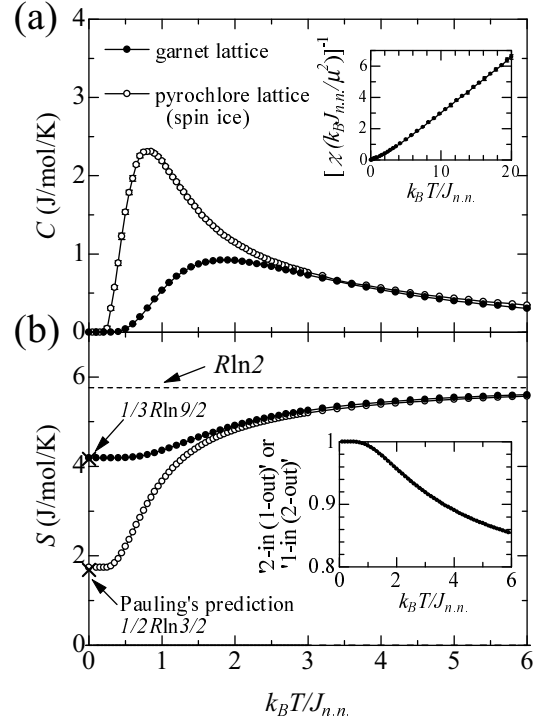


Fig. 2. (a) Specific heat and (b) entropy of the Ising model on the garnet lattice with the nearest-neighbor exchange interaction ($J_s > 0$) as a function of the temperature T . The results for the pyrochlore lattice (spin ice model) is also shown for reference. Inset in (a) shows the inverse of the magnetic susceptibility in the field direction [100], and inset in (b) shows the probability for the configurations of two-in (one-out) or one-in (two-out) to appear. Two crosses are the approximate values of the residual entropy calculated by the method of Pauling:¹⁵ $(1/3)R \ln 9/2$ for the garnet lattice and $(1/3)R \ln 3/2$ for the pyrochlore lattice ($R = k_B N$).

temperatures, all the spin configurations on each triangle, i.e. three-in, three-out, two-in (one-out) and one-in (two-out), are equally populated. As decreasing the temperature, the specific heat features a Schottky-type hump around $k_B T / J_{n.n.} \sim 2$, implying that a high-temperature disordered spin phase gradually changes to the low-temperature phase without any phase transition. Around the crossover temperature, three-in and three-out configurations on each triangle are suppressed with the decrease of the temperature. This is indeed seen in inset of Fig. 2 (b), where the two-in (one-out) or one-in (two-out) spin configuration gets dominant at low temperatures. Correspondingly, the magnetic susceptibility is enhanced, and diverges at absolute zero, as seen in the inset of Fig. 2 (a), which suggests the existence of free spins in the ground state. In fact, Fig. 2 (b) confirms the finite residual entropy at $T = 0$. Therefore, the nearest neighbor Ising model on the garnet lattice has the macroscopic ground-state degeneracy with large residual entropy. These magnetic properties are essentially same

as those for the spin-ice observed in the pyrochlore Ising-spin system.^{1,3,5} As shown in Fig. 2, the residual entropy in the garnet spin system is larger than in the pyrochlore spin system. This may reflect the difference in the number of neighbors, which is smaller in the garnet lattice than in the pyrochlore lattice.

Shown in Figs. 3 and 4 are the data in the presence of a magnetic field. Introducing the field, a new peak structure is developed in the specific heat at low temperatures, because some portion of the ground-state degeneracy is lifted by the applied magnetic field. Since there are several distinct Ising axes in the garnet lattice, the residual entropy takes different values depending on the direction of the applied field, as shown in Fig. 4.

Most of the above properties are similar to those observed for the pyrochlore spin-ice system^{1,5,9-11} except that in the present model the residual entropy is large, and an applied field produces a variety of ground states, which still have macroscopic degeneracy.

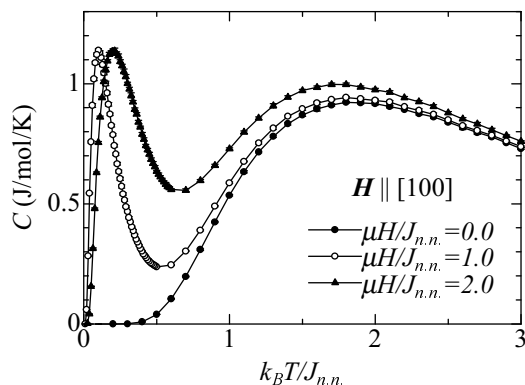


Fig. 3. Specific heat as a function of the temperature for various fields applied along the [100] direction.

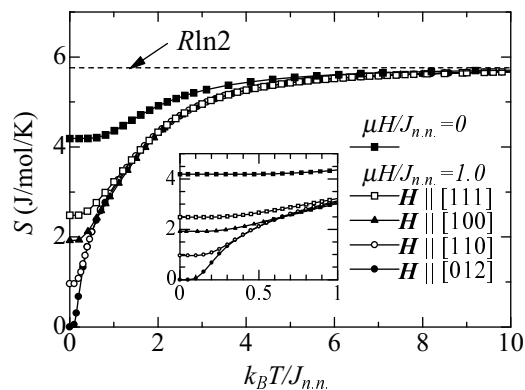


Fig. 4. Entropy as a function of the temperature for the field $H = 1.0$. The exact value of the residual entropy is $S/R = 1/6 \ln 6$, $1/3 \ln 2$, $1/6 \ln 2$ and 0 for the field $\mathbf{H} \parallel [111]$, $[100]$, $[110]$, and $[012]$, respectively. These values are obtained exactly by counting the number of relevant free spins for each case.

3.2 Effects of long-range interaction

Having seen that the model with the nearest neighbor interaction exhibits spin-ice like properties, we now ask how stable the ground state is when the additional interaction among spins is introduced. In fact, according to recent reports for some pyrochlore compounds such as $\text{Dy}_2\text{Ti}_2\text{O}_7$ and $\text{Ho}_2\text{Ti}_2\text{O}_7$, the dipolar interaction may be rather important so as to enhance the tendency to stabilize a magnetically ordered ground state.^{6,16}

In the following, we consider the long-range dipolar interaction to observe the stability of the spin-ice like state against possible ordered states. To analyze the effect of the dipolar interaction systematically, we follow the way of ref.³ and introduce the cutoff n_c to control the effective range of the interaction, where the interactions up to n_c th neighbor spins are taken into account. Although the cutoff has little effect on the phase transition in the pyrochlore system,³ the present garnet lattice system may be more sensitive to the cutoff since the degeneracy of the ground state is much larger than the pyrochlore system.

We study the system with various choices of the cutoff up to $n_c = 20$. The case with $n_c = \infty$ is treated by exploiting a different technique, as will be mentioned later in this section. Since the typical behavior found for the phase transitions is classified into three categories, we show the results for three representative examples by setting the cutoff as $n_c = 4, 5$ and 14, which respectively correspond to the real cutoff distance $l_c/a = 0.56, 0.59$ and 1.0 in unit of the lattice constant a . For a while, we restrict ourselves to the case with $J_s = 0$, and discuss the effect of J_s later in this section.

Before starting the discussions on the phase transitions, we mention here that the models having the interaction with $n_c = 1, 2, 3$ show the spin-ice like behavior analogous to the nearest-neighbor model.

3.2.1 second-order transition ($n_c = 4, 9, 10, 11$)

We start with the results for the model including interaction up to fourth-neighbors ($n_c = 4$) shown in Fig. 5. It is found that two peaks appear at low temperatures besides a much broader hump at higher temperatures around ($k_B T / J_{n.n.} \sim 2$). The higher-temperature hump is essentially the same as that for the model with the nearest neighbor interaction. Therefore, we can see that two peaks at low temperatures are featured by lifting the ground-state degeneracy due to the newly introduced interactions. These two peaks are different in character as seen in the inset of Fig. 5 (a).

The higher-temperature peak seems to show divergent behavior, implying a second-order phase transition. We indeed confirm this by examining the system-size dependence of the specific heat systematically, as shown in Fig. 6. It is found that the increase of the system size enhances the peak and slightly changes the location of the peak. As shown in the inset of Fig. 6, the peak position for each system size satisfies the scaling plot with the Ising critical exponent $\nu = 0.629$. Therefore, we conclude that this phase transition belongs to the universality class of the three-dimensional Ising model,¹⁷ and the critical temperature thus determined is $k_B T_c / J_{n.n.} = 0.418$.

We now wish to ask what kind of order is realized at

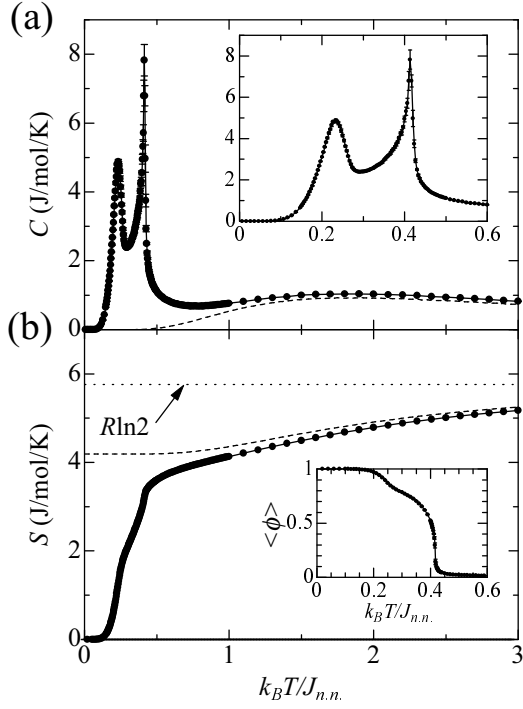


Fig. 5. Specific heat and entropy as a function of the temperature for the model having the interactions up to fourth-neighbors. The specific heat for the nearest-neighbor model is shown as the broken line for reference. Inset in (a) magnifies the specific heat in the low temperature region, and inset in (b) shows the temperature dependence of the order parameter ϕ .

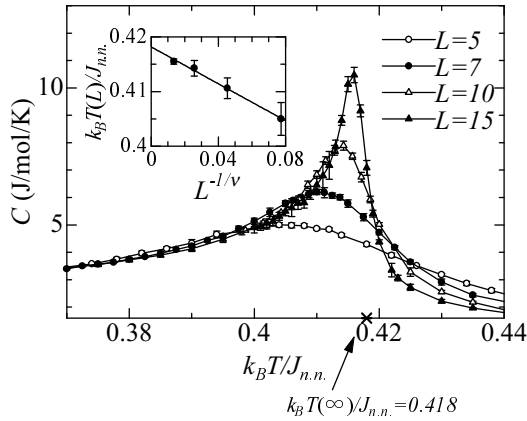


Fig. 6. Specific heat for different choices of the system size. Inset shows the scaling plot of the peak position, which should give the critical temperature in the thermodynamic limit.

this phase transition. We find that the system has the finite order parameter ϕ , which is defined as,

$$\langle \phi \rangle = \frac{1}{4} \left((m_1 - m_2)^2 + (m_2 - m_3)^2 + (m_3 - m_1)^2 + (m_4 - m_5)^2 + (m_5 - m_6)^2 + (m_6 - m_4)^2 \right)^{\frac{1}{2}}, \quad (2)$$

$$m_k = \frac{6}{N} \sum_i \sigma_i, \quad (3)$$

over k th
sublattice

where m_k is the magnetization of the k th sublattice ($k = 1 \sim 6$). In the inset of Fig. 5(b), we show how this order parameter is developed. In order to further clarify the detailed structure of the ordered state, we show the spontaneous magnetization for each sublattice in Fig. 7. The analysis of the magnetization reveals that below the

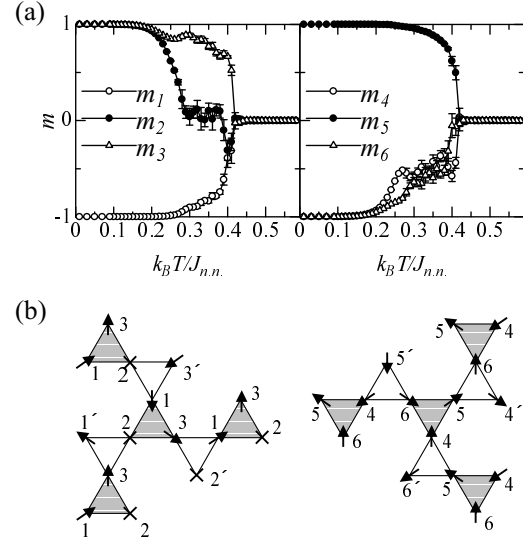


Fig. 7. (a) Spontaneous magnetization for each sublattice m_k as a function of the temperature T . It is seen that just below the critical temperature, the magnetization is not developed for one of six sublattices (lattice 2 in this example). (b) Spin-configuration pattern for the partially disordered phase, where crosses on the lattice 2 mean that spins are still free there.

critical temperature the symmetry breaks only partially, namely, there appears a finite magnetization in five kinds of the sublattices, but no magnetization in the remaining one sublattice. The corresponding spin arrangement is drawn in Fig. 7 (b) schematically. Therefore, we can say that a *partially disordered phase* is realized below the critical temperature ($k_B T / J_{n.n.} < 0.4$). This state is continuously connected to the completely ordered phase realized at zero temperature without any phase transition. This crossover naturally explains why a Schottky-like structure is developed in the specific heat at low temperatures, as observed in Fig. 5. We have confirmed that this type of the second-order transition occurs for the model with $n_c = 4, 9 - 11$.

3.2.2 double second-order transitions ($n_c = 5, 6, 7$)

We next discuss another prototype of phase transition, by taking the $n_c = 5$ case as an example. The analysis can be done in a similar way mentioned above, so that we briefly summarize the relevant points below.

In Fig. 8, we show the results for the specific heat and the entropy. As is the case for the model with $n_c = 4$, the temperature-dependent specific heat has a wide hump at high temperatures, which is supplemented by two peaks at low temperatures. In this case, however, both of the two peaks show divergent behavior, implying that the second-order phase transition takes place

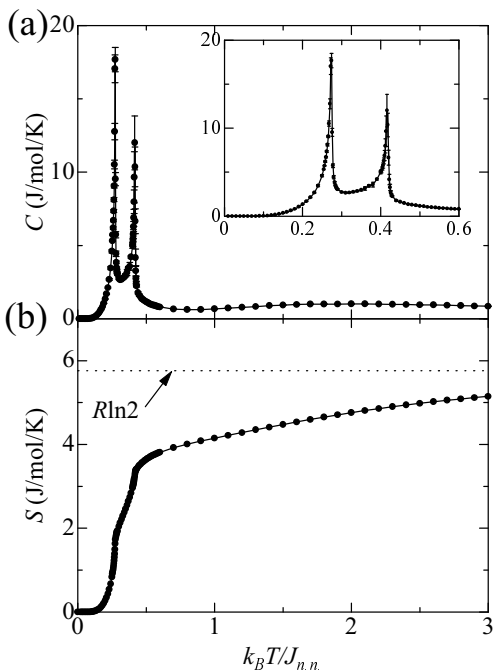


Fig. 8. (a) Specific heat and (b) entropy for the model having the fifth-neighbor interactions ($n_c = 5$).

twice. We would naively expect that the crossover behavior characterized by the lower peak in the $n_c = 4$ case now changes its character to the second-order phase transition. However, it turns out that this simple picture is not correct. By calculating the spontaneous magnetization, we find that in the intermediate phase ($0.27 < k_B T / J_{n.n.} < 0.42$), a partially disordered phase is realized with spin correlations between different sublattices, shown schematically in Fig. 9. Namely, there are specific

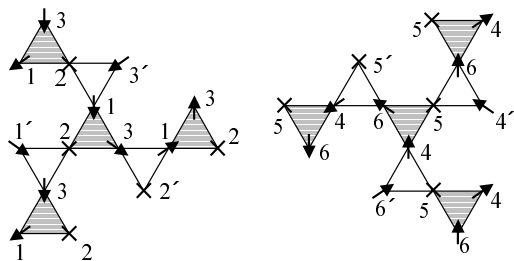


Fig. 9. Spin-configuration pattern of the intermediate ordered phase for the model having the interaction with $n_c = 5$. There are specific correlations between left and right panels (see text).

correlations between the configurations in the left and right panels: for example, if the lattice sites labeled by 2 in the left are disordered, so that the corresponding lattice sites labeled by 5 in the right panel should be disordered. As another example, if we assume the lattice sites labeled by 1 to be disordered, then the lattice sites labeled by 4 should be disordered. As decreasing the temperature, this partially disordered phase is driven to the completely ordered phase via another second-order phase

transition. We have checked that this type of phase transitions are realized for the models with $n_c = 5, 6$ and 7.

3.2.3 first-order transition ($n_c = 8, n_c \geq 12$)

We finally discuss the case exhibiting the first-order phase transition, by taking the case of $n_c = 14$, where the interaction is taken into account up to the fourteenth neighbors.

To see the nature of the first-order phase transition clearly, we first look at the temperature-dependent free energy shown in Fig. 10. As decreasing (increasing) the

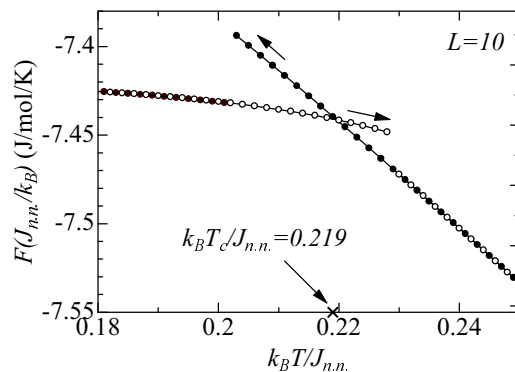


Fig. 10. Free energy F for the Ising model with $n_c = 14$, which clearly shows a cusp singularity. Solid (open) circles represent the results obtained when the temperature is decreased (increased).

temperature from higher (lower) temperatures, the free energy features distinct curves, as is typical for first-order transitions. We note here that in actual Monte Carlo calculations for a finite-size system, there appears hysteresis, which is accompanied by a sudden jump of the free energy at a certain temperature. Nevertheless, we can determine the critical temperature, $k_B T / J_{n.n.} \sim 0.219$, correctly from the crossing point in the free energy curves.

The specific heat and entropy calculated are shown in Fig. 11. In the high temperature region, a broad hump appears again in the specific heat around $k_B T / J_{n.n.} \sim 2$, similarly to the previous two cases, reflecting the crossover from the free spin state to the spin ice state. In the present case, the first-order transition gives rise to the discontinuity at the critical point in the specific heat, the entropy and the order parameter, as seen in Fig. 11. A remarkable point is that the ordered state below the critical temperature has the same order as for the $n_c = 4$ case but not for the $n_c = 5$ case. This is a nontrivial consequence due to the long-range interaction on the frustrated garnet lattice.

We have confirmed that the above type of the first-order phase transition occurs for the model with $n_c = 8$ and $n_c \geq 12$. In this connection, we make a comment on the system with the original dipolar interaction ($n_c = \infty$). Since our technique employed here is not appropriate to treat the $n_c = \infty$ case directly, we have instead used the Ewald method,^{6, 16, 18} which can overcome the above

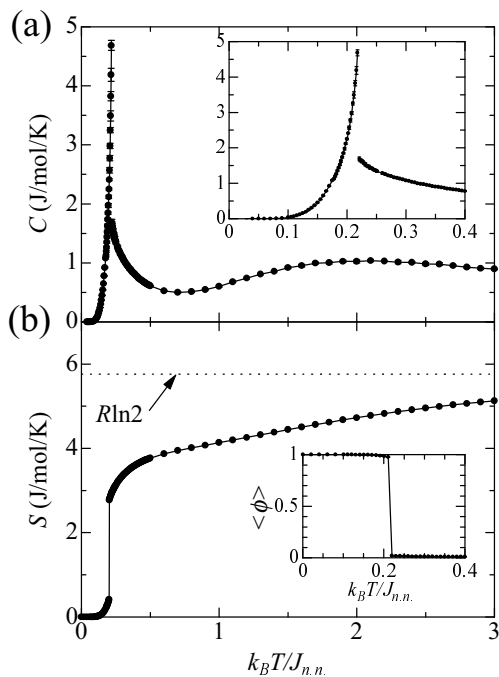


Fig. 11. (a) Specific heat and (b) entropy as a function of the temperature for the system with $n_c = 14$. Inset in (b) shows the temperature dependence of the order parameter $\langle \phi \rangle$.

difficulty. We have found that the first-order transition similar to Fig. 11 indeed occurs even in the $n_c = \infty$ case.

3.3 Phase diagram

We repeat similar calculations by changing the ratio of the exchange interaction and the long-range interaction to discuss the competition between the spin-ice like state and the magnetically ordered states. Here, we make use of the parameter $K = J_{D1}/J_{n.n.}$ with $J_{n.n.} = J_S + J_{D1}$ defined before. We show the phase diagrams obtained for the three prototype cases with $n_c = 4$ and 5, 14 in Fig. 12. As mentioned above, when $K = 0$ ($J_{ij} = 0$), the system is reduced to the Ising model with nearest neighbor interactions. It is seen that the introduction of the long-range interaction has little effect on the spin-ice like behavior at higher temperatures. Namely, the temperature characterizing the crossover is little changed by the long-range interaction. This is because spin-ice like behavior is dominated mainly by local spin fluctuations. On the other hand, the long-range interaction enhances long-range correlations among spins in the same sublattice, inducing the phase transition to several distinct magnetically ordered ground states at low temperatures. In particular, we have obtained partially disordered phases, which are inherent in frustrated Ising systems.^{19–22}

In comparison with the pyrochlore system with the long-range dipolar interaction,³ the present system shows rather complicated phase diagrams, depending on the cutoff distance. This may be related to the fact that the garnet system has much larger residual entropy than that for the pyrochlore system.

In realistic Ising garnet systems, it may be expected that either the spin-ice behavior or the first-order phase

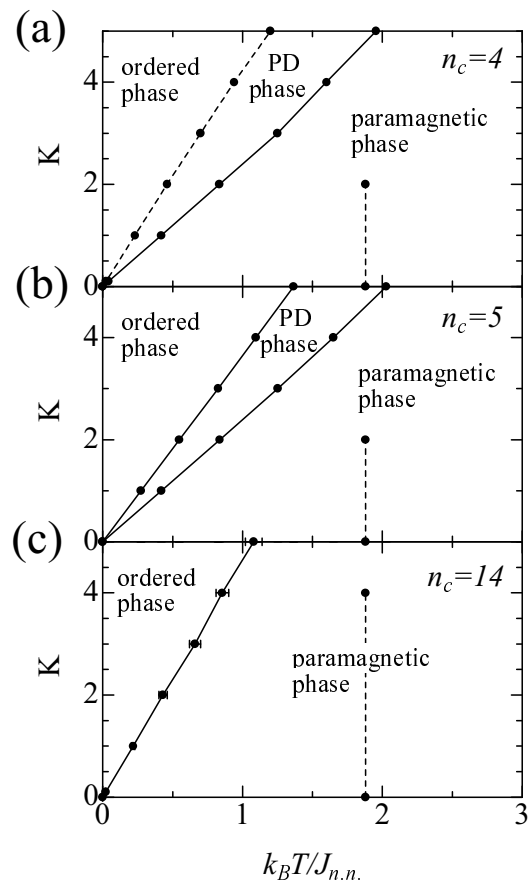


Fig. 12. Phase diagrams for the Ising spin system on the garnet lattice, where the long-range dipolar interaction is taken into account up to $n_c = 4, 5$ and 14 neighbors. Solid lines represent the phase boundary between the magnetically ordered phase and the paramagnetic phase (second-order transition for (a) and (b), and first-order transition for (c)). Dashed lines represent the crossover around which the specific heat exhibits its maximum value.

transition would occur.

4. Summary

We have investigated the classical Ising model on the garnet lattice by means of Monte Carlo simulations with the heat bath algorithm. It has been clarified that the Ising model with nearest neighbor interaction exhibits the spin-ice like behavior without any phase transitions, resulting in the large residual entropy at zero temperature. It has been found that a part of the degeneracy in the ground state is lifted upon introducing a magnetic field. We have also discussed the effect of the dipolar-type interaction to clarify how the spin-ice like state competes with the magnetically ordered states.

We have seen that when the long-range dipolar interaction exists the first-order transition takes place even though the magnitude of the dipolar interaction is small. However, the transition temperature should be very low in such cases, making the spin-ice like behavior dominant in the wide temperature range.

Although the spin ice behavior has not been observed experimentally in the existing garnet compounds, we expect that possible candidates can be synthesized in the

future, which may further stimulate theoretical and experimental investigations in this class of spin-ice systems.

Acknowledgement

This work was partly supported by a Grant-in-Aid from the Ministry of Education, Science, Sports and Culture of Japan.

- 1) A. P. Ramirez, A. Hayashi, R. J. Cava, R. Siddharthan and B. S. Shastry: *Nature* **399**, 333 (1999).
- 2) B. C. den Hertog and M. J. P. Gingras: *Phys. Rev. Lett.* **84**, 3430 (2000).
- 3) R. Siddharthan, B. S. Shastry, A. P. Ramirez, A. Hayashi, R. J. Cava and S. Rosenkranz: *Phys. Rev. Lett.* **83**, 1854 (1999).
- 4) R. Siddharthan, B. S. Shastry and A. P. Ramirez: *Phys. Rev. B* **63**, 184412 (2001).
- 5) M. J. Harris, S. T. Bramwell, P. C. W. Holdsworth and J. D. M. Champion: *Phys. Rev. Lett.* **81**, 4496 (1998).
- 6) R. G. Melko, B. C. den Hertog and Michel J. P. Gingras: *Phys. Rev. Lett.* **87**, 067203 (2001).
- 7) M. J. Harris, S. T. Bramwell, D. F. McMorrow, T. Zeiske and K. W. Godfrey: *Phys. Rev. Lett.* **79**, 2554 (1997).
- 8) S. T. Bramwell, M. J. Harris, B. C. den Hertog, M. J. P. Gingras, J. S. Gardner, D. F. McMorrow, A. R. Wildes, A. L. Cornelius, J. D. M. Champion, R. G. Melko and T. Fennell: *Phys. Rev. Lett.* **87**, 047205 (2001).
- 9) K. Matsuhira, Z. Hiroi, T. Tayama, S. Takagi and T. Sakakibara: *J. Phys. Condens. Matter* **14**, L559 (2002).
- 10) M. Udagawa, M. Ogata and Z. Hiroi: *J. Phys. Soc. Jpn.* **71**, 2365 (2002).
- 11) R. Higashinaka, H. Fukazawa and Y. Maeno: *Phys. Rev. B* **68**, 014415 (2003).
- 12) O. A. Petrenko and D. McK. Paul: *Phys. Rev. B* **63**, 024409 (2000).
- 13) P. Schiffer, A. P. Ramirez, D. A. Huse and A. J. Valentino: *Phys. Rev. Lett.* **73**, 2500 (1994).
- 14) O. A. Petrenko, C. Ritter, M. Yethiraj and D. Mck Paul: *Phys. Rev. Lett.* **80**, 4570 (1998).
- 15) L. Pauling: *The nature of the Chemical Bond* (Cornell, Ithaca, 1960) 3rd ed.
- 16) R. G. Melko, Matthew Enjalran, Byron C. den Hertog and Michel J. P. Gingras: preprint cond-mat/0308282.
- 17) Y. Ozeki and N. Ito: *J. Phys. Soc. Jpn.* **69**, 193 (2000).
- 18) P. P. Ewald: *Ann. Physik* **64**, 253 (1921).
- 19) S. Niitaka, K. Yoshimura, K. Kosuge, M. Nishi and K. Kakurai: *Phys. Rev. Lett.* **87**, 177202 (2001).
- 20) O. Koseki and F. Matsubara: *J. Phys. Soc. Jpn.* **69**, 1202 (2000).
- 21) T. Takagi and M. Mekata: *J. Phys. Soc. Jpn.* **64**, 4609 (1995).
- 22) H. Shiba: *Prog. Theor. Phys.* **28**, 466 (1980).